Quantification of microstructure to reveal the solidification path of an alloy

A-A. Bogno[1], W.Hearn[1], J.E.Spinelli[1, 2], J. Valloton[1], H.Henein[1]
[1] Department of Chemical and Materials Engineering
University of Alberta, Edmonton, AB T6G 2G6 Canada

[2] Department of Materials Engineering, Federal University of São Carlos,
São Carlos, SP 13565-905 Brazil

Email: bogno@ualberta.ca / hhenein@ualberta.ca

Abstract. This paper reports on the development of Solidification Continuous Cooling Transformation diagrams that relate the solidification paths to the inherent microstructures of binary and ternary alloys. The methodology is based on the quantification of a solidified microstructure for its various phase fractions. This measured data is combined with well-established solidification models and phase diagrams to yield undercooling temperatures of individual phases. The thermal history and undercooling of different phases in the solidified alloy are estimated for a wide range of cooling rates (from 10^{-2} °Cs^{-1} to 10^{5} °Cs^{-1}). To describe the methodology, dedicated samples of Al-Cu, Al-Cu-Sc and Al-Si alloys were studied. With said alloys being solidified in a controlled manner, over a wide range of cooling rates and undercoolings, via Impulse Atomization, Electro-Magnetic Levitation, and Differential Scanning Calorimetry

1. Introduction

Cooling rate and undercooling are the most critical process parameters during a solidification process. For some alloys, solidification by cooling too slowly results in the precipitation of undesirable phases or the formation of undesirable phase morphologies. Reactions leading to such outcomes must be avoided in order to achieve optimum properties from the resultant microstructure. For most alloys, when significant undercooling is achieved during solidification, the solid can form using numerous paths from the liquid, yielding a number of possible phases, morphologies, structures and/or supersaturation of solute. Thus, cooling rate must be done as fast as needed coupled with undercooling in order to suppress or promote precipitation of phases and morphologies that are of interest.

The influence of cooling rate and undercooling on the phase transformation behaviour (during solidification) can be described by a solidification continuous cooling transformation (SCCT) diagram. For most industrially relevant metallic alloys, the generated information from such a diagram could be used to optimize the solidification process and thus the properties of the resulting components.

So, as we continue to seek a general way of relating the resultant microstructure to macro-solidification conditions SCCT diagrams could prove a useful asset in alloy and process design. This approach has

been achieved in steels with the development of Continuous Cooling Transformation (CCT) diagrams [1,2]. These CCT diagrams have also been used for aging aluminum alloys[3,4] and for representing the crystallization conditions for bulk metallic glasses [5].
In this work, we propose a methodology to formulate and quantify the solidification paths of binary and ternary alloys with an SCCT diagram. The methodology is based on the quantification of a solidified microstructure for its various phase fractions. This measured data is combined with well-established phase diagrams and solidification models to yield undercooling temperatures of individual phases [6] . The thermal history and undercooling of different phases in the solidified alloy are measured either directly or estimated for a wide range of cooling rates (from 10-2 °Cs-1 to 105 °Cs-1). In this paper, the methodology will be described using examples of Al-Cu, Al-Cu-Sc and Al-Si alloys. For the Al-Cu /Al-Cu-Sc alloys, the effect of Sc is investigated and the precipitation of an undesirable phase is analyzed. For the Al-Si alloy, the variation in the eutectic Si morphology is investigated.

2. **Methodology**

Samples were solidified in a controlled manner, under a wide range of cooling rates and undercoolings, using three very well-known techniques: Impulse Atomization (IA) [7,8], Electro-Magnetic Levitation (EML) [9–11], and Differential Scanning Calorimetry (DSC) [12,13]. In this work, the term cooling rate refers to the cooling rate of the liquid whether in droplet form or in a crucible. DSC is a thermal analysis technique used to determine the amount of energy absorbed or released by a sample as it is heated or cooled inside a crucible. As a non-containerless solidification technique, it yields low nucleation undercooling and its cooling rate (which is directly measureable) is limited to a narrow range (up to 0.8 °C s-1). IA and EML are both containerless solidification techniques that have the ability to induce high nucleation undercooling during solidification. EML generates a single 6 mm diameter droplet per run, which solidifies at relatively low but measurable (via a pyrometer) cooling rates (101 °C s-1), triggered by jets of inert He gas. In comparison, IA generates numerous droplets of various sizes during a single run. The cooling rate in IA is defined by the droplet size and the surrounding cooling gas (He, Ar or N2), and can reach cooling rates up to 105 °C s-1. However, in-situ measurement of the cooling rate in IA is complicated, as the spray of droplets fall within an inert atmosphere with an initial velocity of 0.5ms-1 [7,14]. Consequently, a solidification model for atomization developed by Wiskel et al. [7,14] was used to estimate the cooling rate of each investigated IA droplets.

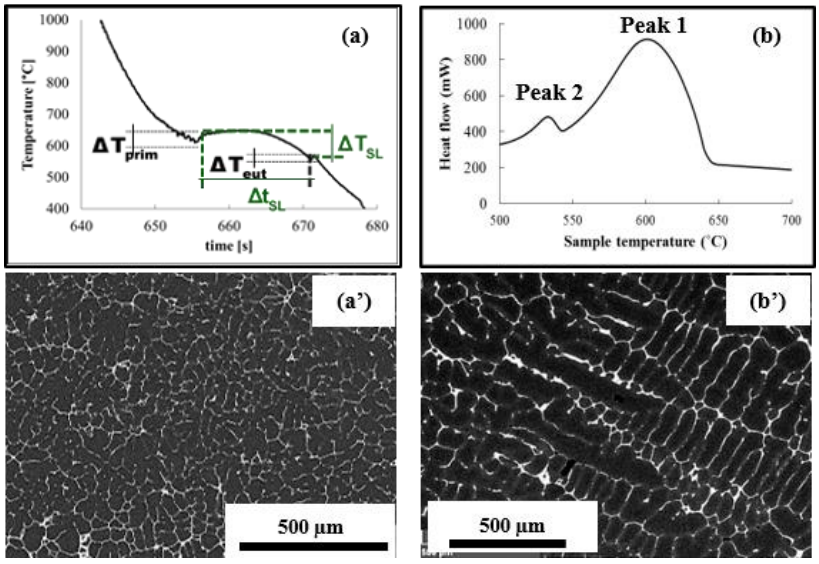

Figure 1: Solidification curve and microstructures of Al-4.5 wt% Cu samples obtained by (a-a') EML with a measured cooling rate of 9.2 ˚Cs^{-1} and primary and eutectic nucleation undercooling ΔT_{prim}

=34˚C and ΔT_{eut}= 13˚C respectively; (b-b') DSC cooling at the rate of 0.8˚Cs^{-1}, peak 1 and peak 2 correspond respectively to the precipitation of primary α-Al and the eutectic structure (α-Al +θ-Al$_2$Cu).

Figure 1 shows cooling curves of the Al-4.5wt% Cu samples solidified using EML and DSC. The corresponding sample micrographs were obtained by Scanning Electron Microscopy (SEM), and the application of backscattered electron (BSE) imaging. Thus, atomic number (Z) contrast was obtained so that α-Al is identified by the dark color while the Cu rich θ-Al$_2$Cu is white.

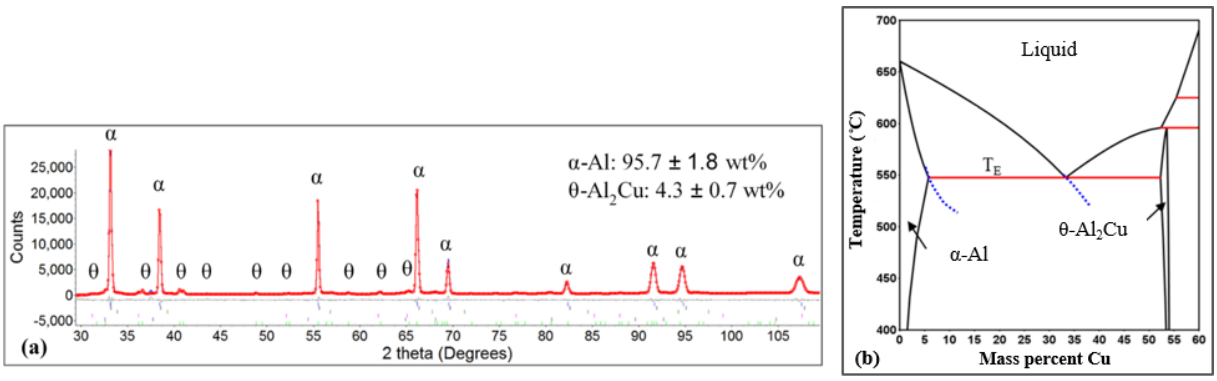

Figure 2: (a) Neutron diffraction diagram of Impulse Atomized droplets of Al-4.5wt% Cu. The phase fractions are obtained by rietveld refinement analysis of the diffraction pattern [15] (b) Al-richer corners of Al-Cu binary phase diagrams. The dashed lines represent the extensions of the solidus and liquidus lines obtained by Thermo-Calc, TTAL7 version 1.1, 2008 [16].

Primary and secondary phase nucleation undercoolings are determined using our new methodology described in [6]. The methodology is based on experimental determination of phase fraction, preferably using a 3D technique such as neutron diffraction (Figure 2). In addition, this methodology includes, secondary dendrite arm spacing (SDAS) measurements, metastable extension of the solidus and liquidus lines of the alloy and a semi-empirical coarsening model that uses the SDAS [17].

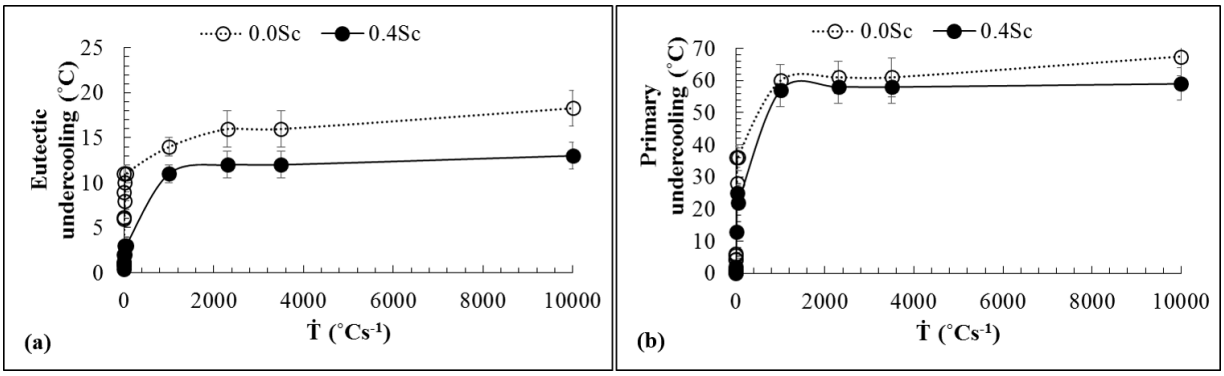

Figure 3: Variation of nucleation undercooling with solidification cooling rate for Al-4.5wt%Cu and Al-4.5wt%-0.4wt%Sc alloys.

Figure 3 shows the variation of primary phase and eutectic nucleation undercooling with cooling rate for the Al-Cu and Al-Cu-Sc alloys. It is worth noting that Sc addition causes a decrease in the nucleation undercooling that is independent of the cooling rate.

3. SCCT diagrams of Al-4.5wt%Cu and Al-4.5wt%Cu-0.4wt%Sc

Temperature, during DSC experiments, is directly measured by thermocouples that are placed underneath the sample and reference crucibles. During EML, the temperature of the sample is recorded

via pyrometry, including the rise of temperature due to the release of solidification latent heat. However, as stated earlier, during IA, direct measurement of the thermal history is difficult to achieve in-situ due to the experimental setup. A numerical model is therefore, used to determine the thermal history of an atomized droplet. The model, based on the quantification of heat exchange between an IA droplet and gas in an inert environment, has been developed from Wiskel's heat transfer model formulation [7] [14] and validated in [8].

Figure 4a and 4b show the solidification continuous cooling transformation (SCCT) curves of the investigated Al-4.5wt%Cu and Al-4.5wt%Cu-0.4wt%Sc which are in preparation for publication [18], respectively. From these results, it can be concluded that both primary phase and eutectic nucleation undercoolings increase as the cooling rate is increased. Also, to avoid the formation of the ternary W-phase, which is reported to be detrimental for Al-Cu-Sc alloys[19]–[25], cooling rates of the order of 101 °Cs-1 or higher are necessary.

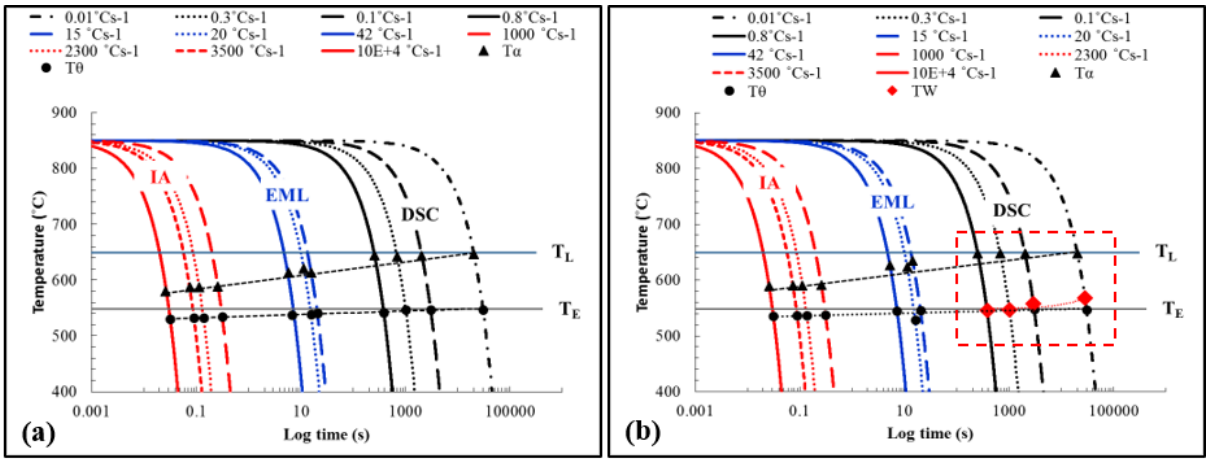

Figure 4: Solidification Continuous Cooling Transformation curves of (a) Al-4.5wt%Cu (b) Al-4.5wt%Cu-0.4wt%Sc. The nucleation temperatures zone of the ternary W-phase is indicated by the square.

4. SCCT diagram of Al-10wt%Si

In recent work by W.Hearn [26] and Hearn et al [27], an Al-10wt%Si alloy, generated by both IA and DSC, was investigated. The transition of Si morphology in this near eutectic Al-Si solidification was analyzed as a function of the liquid cooling rate and the eutectic Si nucleation temperature.

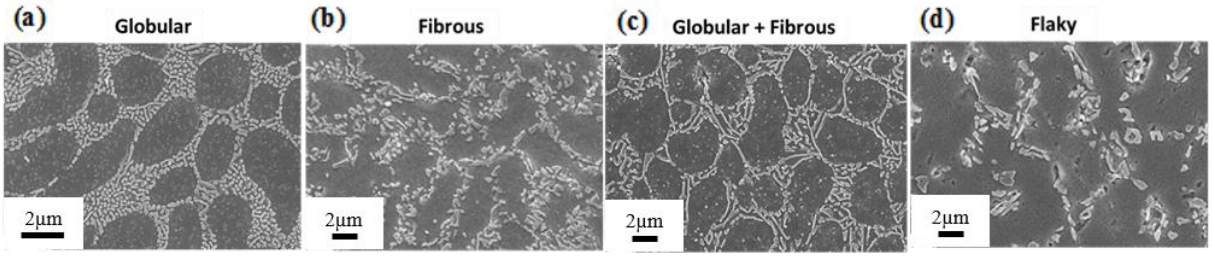

Figure 5: FE-SEM images outlining the four morphologies of the eutectic Si phase that were observed by Hearn [26,27]. (a) "Globular" Si morphology. (b) Fibrous" Si morphology. (c) "Globular + Fibrous" Si morphology. (d) "Flaky" Si morphology.

Figure 5(a through d) shows the four types of Si morphologies observed in W. Hearn's work. Typically, as the cooling rate decreases with the droplet size, the Si morphology will transition from globular → fibrous → flaky. Consequently, an SCCT diagram, shown in Figure 6, was generated in order to correlate

the solidification parameters and the inherent Si morphologies. Thus, the primary and eutectic nucleation temperatures, along with the Si morphology, are shown as a function of liquid cooling rate. From the SCCT diagram it can be seen that, the Si morphology transitions from globular → fibrous → flaky corresponding to the decrease in undercooling with decreasing cooling rate. Also, it is worth mentioning that a more refined Si is obtained as the morphology transitions from flaky to globular.

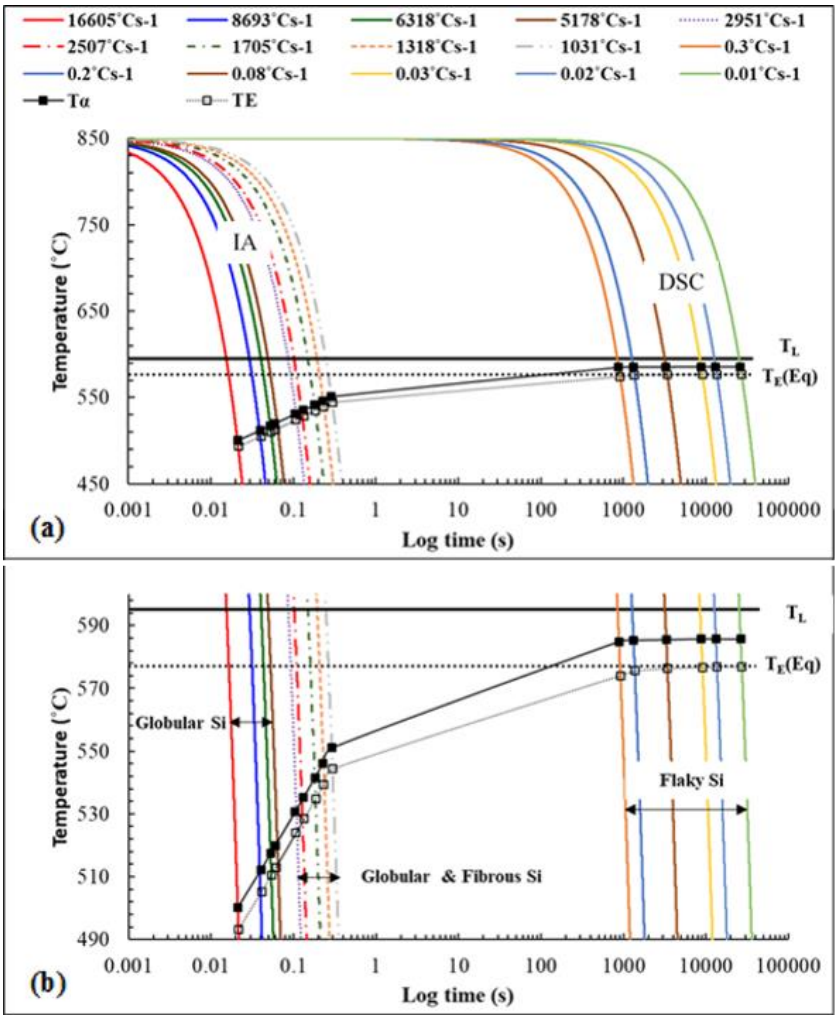

Figure 6: (a) Solidification Continuous Cooling Transformation curves of Al-10Si (b) A zoom on the variation of primary and eutectic nucleation temperature with cooling rate and the corresponding Si morphologies [27].

5. Summary

A new methodology to determine the solidification path of an alloy over a wide range of cooling rates has been presented. The methodology is based on quantitative analysis of the solidification microstructures of samples generated by DSC, EML and IA. Phase fraction measurements were combined with solidification models to determine the nucleation undercooling of individual phases. In this study, Al-Cu, Al-Cu-Sc and Al-Si of hypo-eutectic compositions were investigated. Sc is found to lower the nucleation undercooling and induce the precipitation of the detrimental W-phase at lower cooling rates (<10°Cs-1) and undercooling (<10°C). For the Al-Si alloy, it was found that the Si morphology would transition from flaky →fibrous → globular, where a globular Si morphology was favoured at high cooling rates and undercoolings.

Acknowledgements
The authors express their gratitude to Dimitry Sediako and Ahmed Nawabi for their valuable help during neutron diffraction experiments carried out at the Canadian National Laboratory in Chalk River, Canada. The authors are also grateful to the German Aerospace Center (DLR) and staff for the electromagnetic levitation experiments. The Natural Sciences and Engineering Research Council (NSERC) of Canada and the European Space Agency (ESA) are gratefully acknowledged for their financial support.

References

[1] Xu, G., Wan, L., Yu,S., Liu,L., and Luo,F., 2008, *Mater. Lett.*, **62**, (24), 3978.
[2] Kong,J, and Xie,C., 2006, *Mater. Des.*, **27**, (10), 1169.
[3] Milkereit,B., Wanderka, N., Schick,C.,and Kessler, O., 2012, *Mater. Sci. Eng. A*, **550**, 87.
[4] Kessler, O., von Bargen, R., Hoffmann, F., and Zoch,H.W., 2006, *Mater. Sci. Forum*, **519–521**, 1467.
[5] Schroers, J., Masuhr,A., Busch, R., and Johnson,W.L., 1999, *BULK METALLIC GLASSES*, **554**, 263.
[6] Bogno,A.-A., Khatibi,P.D., Henein,H., and Gandin, Ch-A., 2016, *Metall. Mater. Trans. A Phys. Metall. Mater. Sci.*, **47A,** (9), 4606
[7] Wiskel, J.B., Navel, K., Henein,H., and Maire, E., 2002, *Canadian Metallurgical Quarterly*, **41**, (2), 193.
[8] Prasad, A. Mosbah,S. Henein, H. and Gandin, Ch.-A. 2009, *ISIJ Int.*, **49**, (7), 992.
[9] Liu, R.P., Volkmann, T., and Herlach,D.M., 2001, *Acta Mater.*, **49**, (3), 439.
[10] Tourret,D. Gandin, Ch - A.,Volkmann, T., Herlach, D. M., 2011, *Acta Mater.*, **59**, (17), 6658.
[11] Ilbagi, A., Khatibi,P.D., Henein,H., Gandin, Ch.-A., and Herlach, D.M., 2012, *Int. Conf. 3D Mater. Sci.*, 67.
[12] Hayoune, A., 2013, *Int. J. Mod. Phys. B*, **27**, (20), 1350084.
[13] Gao, Y.L., Zhuravlev,E., Zou,C.D., Yang,B., Zhai,Q.J., and Schick,C., 2009, *Thermochim. Acta*, **482,** (1–2), 1.
[14] Wiskel, J.B., Navel, K., Henein,H., and Maire, E., 2002, *Canadian Metallurgical Quarterly*, **41**, (2), 97.
[15] Young, R.A., *The Rietveld Method*. 1993.
[16] Andersson, J.O., Helander,T., Höglund,L., Shi,P., and Sundman,B., 2002, *Calphad Comput. Coupling Phase Diagrams Thermochem.*, **26**, (2), 273.
[17] Kurz, W., and Fisher,D.J., 1998, *Fundamentals of Solidification*, 4th editio. CRC Press.
[18] Valloton, J., Bogno, A.-A., and Henein, H., Solidification Continuous Cooling Transformation Diagrams of metallic alloys (Manuscript in preparation).
[19] Prasad, A., Mosbah,S., Henein,H., and Gandin,Ch.-A., 2009, *ISIJ International*, **49**, (7), 992.
[20] Røyset,J., 2007., *Metall. Sci. andTechnology*, **25**, (2),11.
[21] Røyset, J., and Ryum,N., 2005, *Int. Mater. Rev.*, **50**, (1), 19.
[22] Norman, A., Prangnell,P., and McEwen,R., 1998, *Acta Mater.*, **46**, (16), 5715.
[23] Bo, H., Liu,L.B., and Jin,Z.P., 2010, *J. Alloys Compd.*, **490**, (1), 318.
[24] Toropova, L.S., Eskin, D.G., Kharakterova,M.L., and Dobatkina, T.V., 1998, *Advances in Aluminum Alloys Containing Scandium*. Amsterdam: Gordon and Breach Science publishers.
[25] Kharakterova, M.L., 1991, *Izv. Akad. Nauk SSSR, Met.*, **4**, 191.
[26] Hearn, W., 2018, "The Microstructure, Morphology and Mechanical Properties of Rapidly Solidified Al-10wt%Si Alloy," University of Alberta.
[27] Hearn, W., Bogno,A.-A., Spinelli, J., Valloton,J., and Henein, H., 2018, *Metall. Mater. Trans. A.,(in press).*